



# Synthesis, Structures and Chemistry of the Metallaboranes of Group 4-9 with M<sub>2</sub>B<sub>5</sub> Core Having a Cross Cluster M-M Bond

Ranjit Bag, Suvam Saha, Rosmita Borthakur, Bijan Mondal, Thierry Roisnel, Vincent Dorcet, Jean-François Halet, Sundargopal Ghosh

## ► To cite this version:

Ranjit Bag, Suvam Saha, Rosmita Borthakur, Bijan Mondal, Thierry Roisnel, et al.. Synthesis, Structures and Chemistry of the Metallaboranes of Group 4-9 with M<sub>2</sub>B<sub>5</sub> Core Having a Cross Cluster M-M Bond. *Inorganics*, 2019, 7 (3), pp.27. 10.3390/inorganics7030027 . hal-02115716

**HAL Id: hal-02115716**

**<https://univ-rennes.hal.science/hal-02115716>**

Submitted on 1 Apr 2020

**HAL** is a multi-disciplinary open access archive for the deposit and dissemination of scientific research documents, whether they are published or not. The documents may come from teaching and research institutions in France or abroad, or from public or private research centers.

L'archive ouverte pluridisciplinaire **HAL**, est destinée au dépôt et à la diffusion de documents scientifiques de niveau recherche, publiés ou non, émanant des établissements d'enseignement et de recherche français ou étrangers, des laboratoires publics ou privés.



## Article

# Synthesis, Structures and Chemistry of the Metallaboranes of Group 4–9 with $M_2B_5$ Core Having a Cross Cluster M–M Bond

Ranjit Bag <sup>1</sup>, Suvam Saha <sup>1</sup>, Rosmita Borthakur <sup>1</sup> , Bijan Mondal <sup>1</sup> , Thierry Roisnel <sup>2</sup> , Vincent Dorcet <sup>2</sup>, Jean-François Halet <sup>2</sup> and Sundargopal Ghosh <sup>1,\*</sup>

<sup>1</sup> Department of Chemistry, Indian Institute of Technology Madras, Chennai 600036, TN, India; mail2ranjitbag@gmail.com (R.B.); suvamsaha10@gmail.com (S.S.); roschem07@gmail.com (R.B.); mondal.bijan@gmail.com (B.M.)

<sup>2</sup> Univ Rennes, CNRS, ISCR (Institut des Sciences Chimiques de Rennes)-UMR 6226, F-35000 Rennes, France; thierry.roisnel@univ-rennes1.fr (T.R.); vincent.dorcet@univ-rennes1.fr (V.D.); jean-francois.halet@univ-rennes1.fr (J.-F.H.)

\* Correspondence: sghosh@iitm.ac.in; Tel.: +91-44-22574230

Received: 29 January 2019; Accepted: 14 February 2019; Published: 26 February 2019



**Abstract:** In an attempt to expand the library of  $M_2B_5$  bicapped trigonal-bipyramidal clusters with different transition metals, we explored the chemistry of  $[Cp^*WCl_4]$  with metal carbonyls that enabled us to isolate a series of mixed-metal tungstaboranes with an  $M_2\{B_4M'\}$  ( $M = W$ ;  $M' = Cr(CO)_4$ ,  $Mo(CO)_4$ ,  $W(CO)_4$ ) core. The reaction of in situ generated intermediate, obtained from the low temperature reaction of  $[Cp^*WCl_4]$  with an excess of  $[LiBH_4 \cdot thf]$ , followed by thermolysis with  $[M(CO)_5 \cdot thf]$  ( $M = Cr, Mo$  and  $W$ ) led to the isolation of the tungstaboranes  $[(Cp^*W)_2B_4H_8M(CO)_4]$ , **1–3** (**1**:  $M = Cr$ ; **2**:  $M = Mo$ ; **3**:  $M = W$ ). In an attempt to replace one of the BH—vertices in  $M_2B_5$  with other group metal carbonyls, we performed the reaction with  $[Fe_2(CO)_9]$  that led to the isolation of  $[(Cp^*W)_2B_4H_8Fe(CO)_3]$ , **4**, where  $Fe(CO)_3$  replaces a  $\{BH\}$  core unit instead of the  $\{BH\}$  capped vertex. Further, the reaction of  $[Cp^*MoCl_4]$  and  $[Cr(CO)_5 \cdot thf]$  yielded the mixed-metal molybdaborane cluster  $[(Cp^*Mo)_2B_4H_8Cr(CO)_4]$ , **5**, thereby completing the series with the missing chromium analogue. With 56 cluster valence electrons (cve), all the compounds obey the cluster electron counting rules. Compounds **1–5** are analogues to the parent  $[(Cp^*M)_2B_5H_9]$  ( $M = Mo$  and  $W$ ) that seem to have generated by the replacement of one  $\{BH\}$  vertex from  $[(Cp^*W)_2B_5H_9]$  or  $[(Cp^*Mo)_2B_5H_9]$  (in case of **5**). All of the compounds have been characterized by various spectroscopic analyses and single crystal X-ray diffraction studies.

**Keywords:** chromaborane; metallaborane; mixed-metal cluster; molybdaborane; tungstaborane

## 1. Introduction

Metallaboranes are a class of compounds intermediate between borane cages on one side and transition metal clusters on the other [1–22]. Thus, they provide a platform for the evaluation of electronic compatibility or incompatibility of metal and borane fragments. One of the most studied and explored cluster systems in metallaborane chemistry is the  $M_2B_5$  system reported by us [23–33] and others [34–41]. Earlier, Fehlner and co-workers showed an attractive route for the synthesis of electronically unsaturated metallaboranes, i.e., those, which are formally electron deficient with respect to the number of skeletal electron pairs (sep), required to maintain the observed molecular geometry [34–36,42,43]. This synthetic utility is derived from the tendency of the unsaturated cluster to react with fragments, which can readily donate further electrons to the cluster framework. For example,  $[(Cp^*Cr)_2B_5H_9]$  was synthesized by treating  $[(Cp^*Cr)_2B_4H_8]$  with  $\{BH\}$  sources [35,36]. Following a

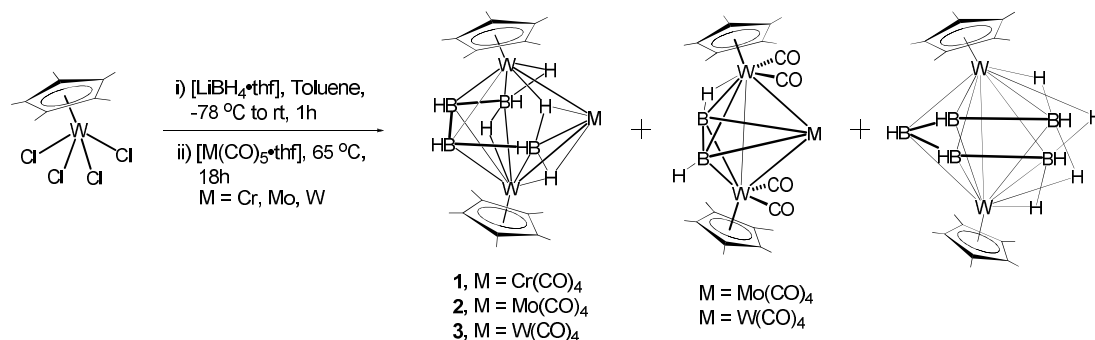
similar procedure molybdenum and tungsten analogues were isolated by the same group followed by the chlorinated rhenium analogue  $[(\text{Cp}^*\text{ReH})\text{B}_5\text{Cl}_5]$  [37–40]. Later in 2008 our group was successful in synthesizing a tantalum analogue, namely  $[(\text{Cp}^*\text{Ta})_2\text{B}_5\text{H}_{11}]$  from the reaction of  $[\text{Cp}^*\text{TaCl}_4]$  with  $\text{LiBH}_4 \cdot \text{thf}$  and  $\text{BH}_3 \cdot \text{thf}$  in toluene under thermolytic condition [23]. Following this, a vanadaborane  $[(\text{Cp}^*\text{V})_2\text{B}_5\text{H}_{11}]$  was isolated under similar reaction conditions [30].

As part of our continuous interest on metallaborane chemistry of group 4–9 transition metals [23–33,44–50], we have synthesized a variety of metallaboranes by cluster expansion reactions using transition metal carbonyls or small organic molecules [46,47,51]. Recently, we have reported an account of the chemistry of Mo system with group 6 metal carbonyls that generated several  $[(\text{Cp}^*\text{Mo})_2\text{B}_5\text{H}_9]$  derivatives in which one of the  $\{\text{BH}\}$  vertices have been replaced by either  $\text{Cp}^*\text{M}$  or metal carbonyl fragments [49]. Apart from their significant geometries, these molecules were found to show interesting bonding interactions, as well as electronic structures. Looking at the geometry of the molybdenum systems, tungsten and chromium systems became of interest. Thus, we were interested to see whether the chemistry associated with a  $\{\text{Cp}^*\text{W}\}$  fragment would mimic  $\{\text{Cp}^*\text{Mo}\}$  or display other interesting variations. Thus, we performed the reaction of an in situ generated intermediate, obtained from the low temperature reaction of  $[\text{Cp}^*\text{WCl}_4]$  with an excess of  $[\text{LiBH}_4 \cdot \text{thf}]$ , followed by thermolysis with  $[\text{M}(\text{CO})_5 \cdot \text{thf}]$  ( $\text{M} = \text{Cr}, \text{Mo}$  and  $\text{W}$ ) that indeed led to the formation of  $[(\text{Cp}^*\text{W})_2\text{B}_4\text{H}_8\text{Cr}(\text{CO})_4]$ , **1**,  $[(\text{Cp}^*\text{W})_2\text{B}_4\text{H}_8\text{Mo}(\text{CO})_4]$ , **2** and,  $[(\text{Cp}^*\text{W})_2\text{B}_4\text{H}_8\text{W}(\text{CO})_4]$ , **3**. Besides group 6 metal carbonyls, we were also interested to replace the B–H fragments of  $\text{B}_5$  core using other metal carbonyl fragments. Thus, we performed the same chemistry using  $[\text{Fe}_2(\text{CO})_9]$  that led to the isolation of an interesting mixed-metal tungstaborane,  $[(\text{Cp}^*\text{W})_2\text{B}_4\text{H}_8\text{Fe}(\text{CO})_3]$ , **4**. In this report we describe the chemistry of both tungsten and molybdenum derivatives. In addition, we also provide a complete overview of the  $\text{M}_2\text{B}_5$  system of group 4–9 metals.

## 2. Results and Discussion

### 2.1. Synthesis and Characterization of Tungstaboranes $[(\text{Cp}^*\text{W})_2\text{B}_4\text{H}_8\text{M}(\text{CO})_4]$ , **1–3** (**1**: $\text{M} = \text{Cr}$ ; **2**: $\text{M} = \text{Mo}$ ; **3**: $\text{M} = \text{W}$ )

As shown in Scheme 1, the reaction of in situ generated intermediate, obtained from the low temperature reaction of  $[\text{Cp}^*\text{WCl}_4]$  with an excess of  $[\text{LiBH}_4 \cdot \text{thf}]$ , followed by thermolysis with  $[\text{M}(\text{CO})_5 \cdot \text{thf}]$  ( $\text{M} = \text{Cr}, \text{Mo}$  and  $\text{W}$ ) yielded the air and moisture sensitive brown solids **1**, **2** and **3** along with the reported compounds  $[(\text{Cp}^*\text{W}(\text{CO})_2)_2\text{B}_2\text{H}_2\text{M}(\text{CO})_4]$ , ( $\text{M} = \text{Mo}; \text{W}$ ) [50] and  $[(\text{Cp}^*\text{W})_2\text{B}_5\text{H}_9]$  [40] in moderate yields. The  $^{11}\text{B}\{^1\text{H}\}$  nuclear magnetic resonance (NMR) spectrum of compound **1** showed four signals at  $\delta = 70.2, 62.2, 36.5$  and  $25.0$  ppm in 1:1:1:1 ratio indicating the presence of four boron atoms. A similar pattern of  $^{11}\text{B}\{^1\text{H}\}$  NMR was also observed for the molybdaborane  $[(\text{Cp}^*\text{Mo})_2(\mu\text{-H})_2(\mu_3\text{-H})_2\text{B}_4\text{H}_4\text{W}(\text{CO})_4]$  [49]. The  $^1\text{H}$  NMR spectrum showed four signals in the upfield region, which signifies the presence of four different types of W–H–B protons. Further, the  $^1\text{H}$  NMR rationalizes the presence of  $\text{Cp}^*$  ligand. The  $^{11}\text{B}\{^1\text{H}\}$  and  $^1\text{H}$  NMR of **2** and **3** nearly resemble that of **1**, with the four non-equivalent of boron atoms, one chemically equivalent  $\text{Cp}^*$  ligand and four different types of W–H–B protons. The infrared (IR) spectra of **1**, **2** and **3** showed the stretching frequencies corresponding to the CO ligands and  $\text{BH}_t$ . Further, the ESI-MS (HR MS) showed a close association among compounds **2** and **3**.



**Scheme 1.** Synthesis of the tungstaboranes 1–3.

In order to confirm the spectroscopic assignments and to determine the solid-state structures of 1–3, X-ray structure analyses were undertaken. The solid-state structures of 1–3, shown in Figure 1, are consistent with the observed spectroscopic data. The asymmetric unit of 1 contains two independent molecules (one is shown in Figure 1), having similar geometric parameters. Although, the bridging hydride ligands and the B–H terminal hydrogen atoms could not be located in the solid state X-ray structure, their positions were fixed based on <sup>1</sup>H NMR spectroscopy, as shown in Scheme 1. The core geometry of 1–3 is very similar to our recently reported molybdaboranes [(Cp\*Mo)<sub>2</sub>(μ-H)<sub>2</sub>(μ<sub>3</sub>-H)<sub>2</sub>B<sub>4</sub>H<sub>4</sub>W(CO)<sub>4</sub>] and [(Cp\*Mo)<sub>2</sub>(μ-H)<sub>2</sub>B<sub>4</sub>H<sub>4</sub>W(CO)<sub>5</sub>] [49]. If the classical skeletal electron counting formalism [52–54] is applied, the 6-sep clusters 1–3 can be viewed as electron-deficient *nido* species derived from an 8-vertex *oblato-closo* hexagonal bipyramidal cluster, with a cross cluster M–M bond [34–36]. Alternatively, these 6-sep species can be seen as adopting a trigonal bipyramidal geometry in which the central [W<sub>2</sub>B<sub>3</sub>] unit is capped by {BH<sub>3</sub>} and a group 6 metal carbonyl fragment ([Cr(CO)<sub>4</sub>] for 1, [Mo(CO)<sub>4</sub>] for 2 and [W(CO)<sub>4</sub>] for 3) at the two [W<sub>2</sub>B] triangular faces. The W–W bond distances in 1–3 and [(Cp\*W)<sub>2</sub>B<sub>5</sub>H<sub>5</sub>(μ-H)<sub>4</sub>] are comparable (*ca.* 2.84 Å for 1–3; 2.82 Å for [(Cp\*W)<sub>2</sub>B<sub>5</sub>H<sub>5</sub>(μ-H)<sub>4</sub>]) (Table 1). Compounds 1–3 are thus analogous to [(Cp\*W)<sub>2</sub>B<sub>5</sub>H<sub>5</sub>(μ-H)<sub>4</sub>] possessing 56 cve (6 sep) and obey the usual electron counting rules [52–54].

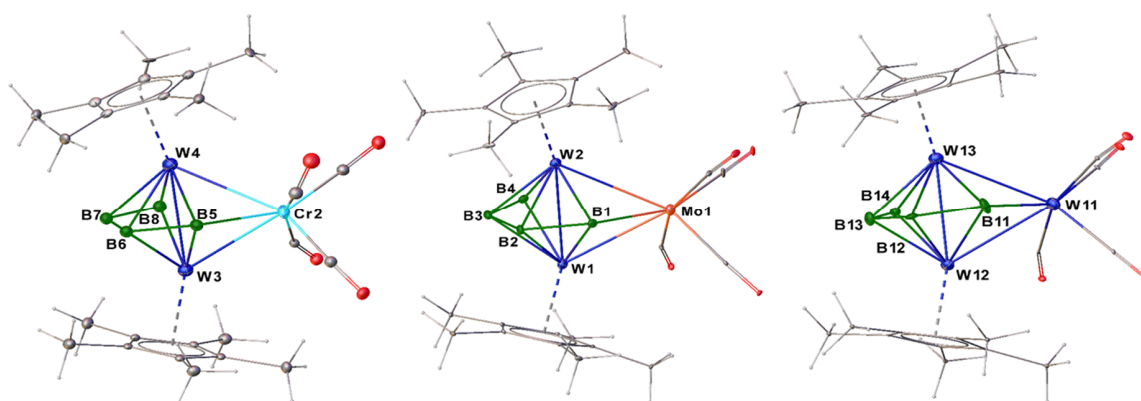


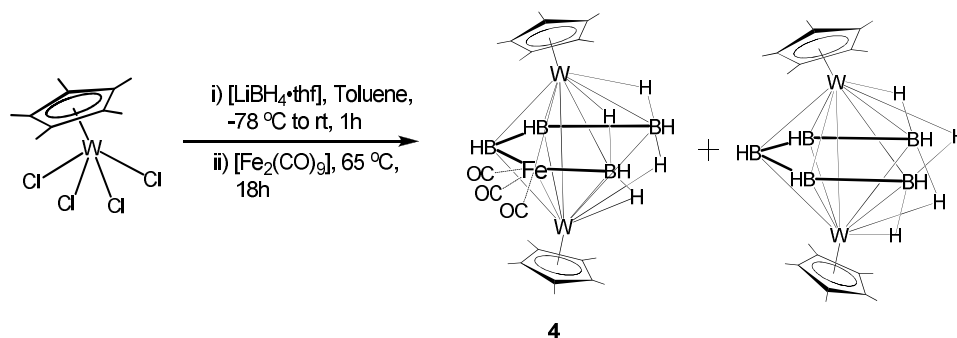
**Figure 1.** Molecular structures and labeling diagrams of 1, 2 and 3. Bridging hydride ligands and hydrogen atoms attached to the boron atoms could not be located. Selected bond lengths (Å) and bond angles (°): 1: W3–W4 2.824(3), Cr2–W3 2.869(9), Cr2–W4 2.895(10), B5–Cr2 2.32(9), B6–B7 1.67(11), B7–B8 1.79(11), B6–W3 2.15(9), B5–W4 2.27(7), B5–W3 2.43(8), W3–Cr2–W4 58.7(2), B7–B6–B5 129(6), W4–B5–W3 74(2), Cr2–B5–W3 74(2), B6–B5–Cr2 125(4). 2: W1–B2 2.200(7), W1–B4 2.325(7), W1–W2 2.8420(4), W1–Mo1 2.9859(6), W2–B1 2.219(7), W2–Mo1 3.0422(6), B1–B2 1.749(10), B2–B3 1.697(11), W4–Mo2 3.0152(7), Mo2–B11 2.439(8), B2–W1–B3 45.0(3), B2–W1–W2 50.28(19), B2–W1–Mo1 95.23(18), W2–W1–Mo1 62.876(13). 3: W12–W13 2.831(10), W12–W11 2.961(10), W12–B11 2.35(3), W12–B12 2.20(2), W12–B13 2.19(2), W13–B14 2.28(2), W13–B11 2.20(2), B11–B12 1.75(3), B12–B13 1.66(3), B13–B14 1.73(3); W12–W11–W13 56.54(2), B11–W12–B12 45.0(9), B11–B12–B13 123.9(18), W12–B11–W13 76.9(9).

**Table 1.** Selected structural parameters and chemical shifts ( $^1\text{H}$  and  $^{11}\text{B}$  NMR) of metallaboranes 1–5 and other related clusters.

Metallaborane	Avg. <i>d</i> [M–M] (Å)	Avg. <i>d</i> [M–B] (Å)	Avg. <i>d</i> [B–B] (Å)	$^{11}\text{B}$ NMR (ppm)	Ref.
$[(\text{Cp}^*\text{Cr})_2\text{B}_4\text{H}_8\text{Fe}(\text{CO})_3]$	2.71	2.15	1.72	–	[34]
$[(\text{Cp}^*\text{Cr})_2\text{B}_4\text{H}_7\text{Co}(\text{CO})_3]$	2.69	2.13	1.69	–	[35]
$[(\text{Cp}^*\text{W})_2\text{B}_5\text{H}_5(\mu\text{-H})_4]$	2.82	2.26	1.71	49.2, 46.9, 26.8	[40]
$[(\text{Cp}^*\text{Mo})_2(\mu\text{-H})_2(\mu_3\text{-H})_2\text{B}_4\text{H}_4\text{W}(\text{CO})_4]$	2.91	2.24	1.72	27.9, 41.9, 81.2	[49]
$[(\text{Cp}^*\text{Mo})_2(\mu\text{-H})_2\text{B}_4\text{H}_4\text{W}(\text{CO})_5]$	2.91	2.24	1.73	103.0, 77.9, 77.0	[49]
$[(\text{Cp}^*\text{W})_2(\mu\text{-H})_2(\mu_3\text{-H})_2\text{B}_4\text{H}_4\text{Cr}(\text{CO})_4]$ , <b>1</b>	2.84	2.38	1.73	70.6, 62.2, 36.5, 25.0	This work
$[(\text{Cp}^*\text{W})_2(\mu\text{-H})_2(\mu_3\text{-H})_2\text{B}_4\text{H}_4\text{Mo}(\text{CO})_4]$ , <b>2</b>	2.83	2.27	1.71	70.1, 60.1, 39.1, 25.6	This work
$[(\text{Cp}^*\text{W})_2(\mu\text{-H})_2(\mu_3\text{-H})_2\text{B}_4\text{H}_4\text{W}(\text{CO})_4]$ , <b>3</b>	2.89	2.24	1.71	70.2, 60.1, 35.5, 26.1	This work
$[(\text{Cp}^*\text{W})_2(\mu\text{-H})_2(\mu_3\text{-H})_2\text{B}_4\text{H}_4\text{Fe}_2(\text{CO})_3]$ , <b>4</b>	2.82	2.28	1.74	79.0, 76.2, 41.0, 35.9	This work
$[(\text{Cp}^*\text{Mo})_2(\mu\text{-H})_2(\mu_3\text{-H})_2\text{B}_4\text{H}_4\text{Cr}(\text{CO})_4]$ , <b>5</b>	2.82	2.23	1.72	83.5, 81.3, 41.3, 27.1	This work

## 2.2. Synthesis and Characterization of Mixed Metal Tungstaborane $[(\text{Cp}^*\text{W})_2\text{B}_4\text{H}_8\text{Fe}(\text{CO})_3]$ , **4**

After successfully isolating clusters 1–3 with group 6 metal carbonyls, we were interested to explore similar chemistry with other metal carbonyls. In this context, we performed the reaction with group 8 metal carbonyls. As shown in Scheme 2, the reaction of in situ generated intermediate, obtained from the low temperature reaction of  $[\text{Cp}^*\text{WCl}_4]$  with an excess of  $[\text{LiBH}_4\cdot\text{thf}]$ , followed by thermolysis with  $[\text{Fe}_2(\text{CO})_9]$  yielded the air and moisture sensitive brown solid, **4** in moderate yield. The  $^{11}\text{B}\{^1\text{H}\}$  NMR of compound **4** displayed four resonances at  $\delta = 79.0, 76.2, 41.0$ , and  $35.8$  ppm, that rationalize the presence of four different boron environments. In addition to the resonances for  $\text{BH}_t$  protons, the  $^1\text{H}$  NMR spectrum showed a signal at  $\delta = 2.24$  ppm corresponding to the  $\text{Cp}^*$  ligands and two upfield signals at  $\delta = -6.97$  and  $-12.92$  ppm, that are probably due to  $\text{W-H-B}$  protons. The presence of CO ligands is confirmed by the IR spectrum. The mass spectrum of **4** showed a molecular ion peak at  $m/z$  853.1456.

**Scheme 2.** Synthesis of the tungstaborane **4**.

The framework geometry of **4** was established by its solid-state structure determination. As shown in Figure 2, it depicts a bicapped trigonal bipyramidal geometry, in which the  $\{\text{W}_2\text{B}_2\text{Fe}\}$  trigonal bipyramid core is capped by the boron atoms B42 and B41 at the triangular  $\{\text{W}_2\text{B}\}$  and  $\{\text{W}_2\text{Fe}\}$  faces similar to compounds 1–3. One of the major difference is the position of the  $\text{Fe}(\text{CO})_3$  unit in the molecule. While in 1–3 the metal carbonyl fragment caps one of the  $\{\text{W}_2\text{B}\}$  triangular faces, in compound **4** it is part of the triangular faces with tungsten  $\{\text{W}_2\text{Fe}\}$ . The geometry of compound **4** resembles that of the tungsten-ruthenium complex  $[(\text{Cp}^*\text{W})_2\text{B}_4\text{H}_8\text{Ru}(\text{CO})_3]$  [33] where  $\text{Ru}(\text{CO})_3$  occupies the same position as that of  $\text{Fe}(\text{CO})_3$ . The W–W bond distance in **4** is comparable to that of 1–3. This type of  $\text{M}_2\text{B}_5$  molecule is rare. With 56 cve (6 sep), compound **4** also obeys the electron counting rules and is an analog of  $[(\text{Cp}^*\text{W})_2\text{B}_5\text{H}_5(\mu\text{-H})_4]$ .

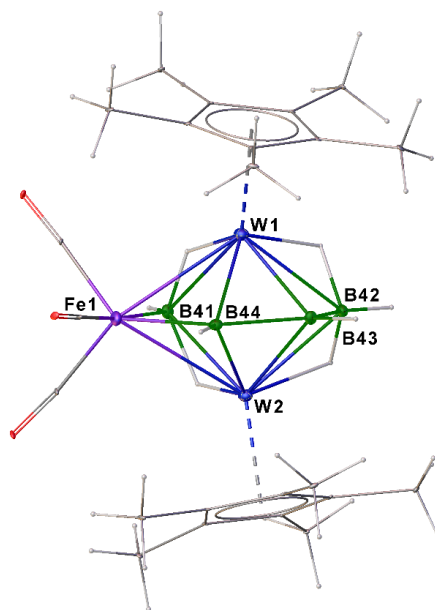
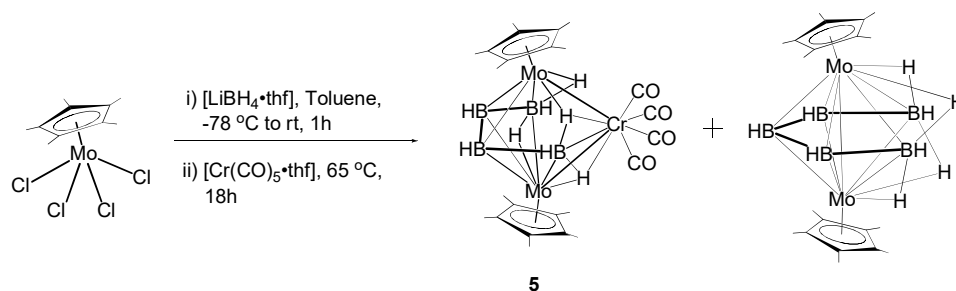


**Figure 2.** Molecular structure and labeling diagram of **4**. Selected bond lengths (Å) and bond angles (°) W1–W2 2.816(4), W1–Fe1 2.667(10), W2–Fe1 2.702(9), W1–B41 2.377(7), W1–B43 2.175(7), W2–B41 2.355(7), W2–B44 2.208(7), B42–B43 1.751(12), B43–B44 1.723(10), Fe1–B44 2.067(7); W1–Fe1–W2 63.28(2), W2–B41–W1 73.1(2), B41–Fe1–B44 97.4(3), B42–B43–B44 124.0(6), Fe1–B44–B43 131.4(5).

### 2.3. Synthesis and Characterization of the Molybdaborane [(Cp\*Mo)<sub>2</sub>B<sub>4</sub>H<sub>8</sub>Cr(CO)<sub>4</sub>], **5**

Recently, we were successful in isolating various mixed-metal molybdaboranes [49,50] by treating the intermediate, obtained from the reaction of Cp\*MoCl<sub>4</sub> and LiBH<sub>4</sub>, with [W(CO)<sub>5</sub>·thf]. Following the same procedure we performed the reaction with [Cr(CO)<sub>5</sub>·thf] and as expected, the reaction enabled us to isolate compound **5** (Scheme 3). Details of its spectroscopic and structural characterization are discussed below.



**Scheme 3.** Synthesis of the mixed-metal molybdaborane cluster **5**.

Compound **5** was obtained as a green solid in moderate yield along with the known compound [(Cp\*Mo)<sub>2</sub>B<sub>5</sub>H<sub>9</sub>] [37,38]. The <sup>11</sup>B{<sup>1</sup>H} NMR spectrum of **5** resembles that of **1–4** with four distinct boron environments at  $\delta$  = 83.5, 81.3, 41.3, and 27.1 ppm. The <sup>1</sup>H NMR spectrum shows four signals in the upfield region, which signifies the presence of four different types of hydride ligands ( $\delta$  = −6.48, −10.56, −11.89, −15.42 ppm). Further, the <sup>1</sup>H NMR rationalizes the presence of one equivalent Cp\* ligand. Presence of the CO ligands was confirmed by IR measurements. The ESI-MS (HR SM) showed a molecular ion peak at  $m/z$  [(M + Na)<sup>+</sup>] = 705.0523, which corresponds to the molecular formula C<sub>24</sub>H<sub>38</sub>B<sub>4</sub>O<sub>4</sub>Mo<sub>2</sub>CrNa.

To confirm the spectroscopic assignments, an X-ray crystallographic analysis was undertaken. The core geometry of **5** is similar to the recently reported molybdaboranes [(Cp\*Mo)<sub>2</sub>(μ-H)<sub>2</sub>(μ<sub>3</sub>-H)<sub>2</sub>B<sub>4</sub>H<sub>4</sub>W(CO)<sub>4</sub>] and [(Cp\*Mo)<sub>2</sub>(μ-H)<sub>2</sub>B<sub>4</sub>H<sub>4</sub>W(CO)<sub>5</sub>] [49]. The asymmetric unit



of **5** contains two independent molecules, which differ slightly in terms of geometric parameters (one is shown in Figure 3). Although, the bridging hydride ligands could not be located in the solid-state X-ray structure, their positions were fixed based on  $^1\text{H}$  NMR, as shown in Scheme 3. With 6 sep, it adopts the expected trigonal bipyramidal geometry in which the central  $[\text{Mo}_2\text{B}_3]$  unit is capped by  $\{\text{BH}_3\}$  and the chromium carbonyl fragment  $[\text{Cr}(\text{CO})_4]$  at the two  $[\text{Mo}_2\text{B}]$  triangular faces. The Mo–Mo bond distance is in accordance with the reported mixed molybdaboranes (Table 1). Compound **5** is thus an additional entry to the class of mixed-metal molybdaborane clusters.

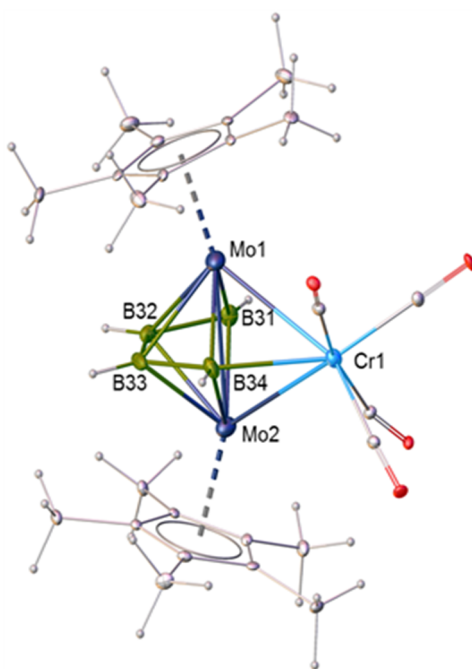


**Figure 3.** Molecular structure and labeling diagram of **5**. Bridging hydride ligands could not be located. Selected bond lengths (Å) and bond angles ( $^\circ$ ) **5**: Mo1–Mo2 2.821(9), Mo1–Cr1 2.923(13), B31–B32 1.733(14), B32–B33 1.706(14), B33–B34 1.723(13), B31–Mo1 2.245(10); Mo1–Cr1–Mo2 57.9(3), Mo1–B311–Mo2 76.4(3), B31–B32–B33 118.4.

In metallaborane chemistry, the mutually synergistic interactions of metal and organic ligands can generate molecules with interesting and diverse geometries. As evident in Table 2, it was shown earlier that group 4 metals from the reaction of  $[\text{Cp}_2\text{MCl}_2]$  ( $\text{M} = \text{Zr}, \text{Hf}$ ) with  $\text{LiBH}_4$  and  $[\text{BH}_3 \cdot \text{thf}]$  generated fused clusters  $[(\text{Cp}_2\text{M})_2\text{B}_5\text{H}_{11}]$  ( $\text{M} = \text{Zr}/\text{Hf}$ ) [55,56] where two *arachno*- $\text{ZrB}_3$  moieties are fused with the  $\text{B}_3$  unit. As expected according to Mingos's formalism it possesses an electron count of 54 cve. Under similar reaction conditions group 5 metals vanadium and tantalum give  $[(\text{CpV})_2\text{B}_5\text{H}_{11}]$  [30] and  $[(\text{Cp}^*\text{Ta})_2\text{B}_5\text{H}_{11}]$  [23] respectively, with a geometry that resembles a *nido* hexagonal bipyramid with a single missing equatorial vertex. A similar structural interpretation has been suggested for the  $[(\text{Cp}^*\text{M})_2\text{B}_5\text{H}_9]$  systems ( $\text{M} = \text{Cr}$  [34–36],  $\text{Mo}$  [37,38], and  $\text{W}$  [40]), as well as for  $[(\text{Cp}^*\text{ReH})_2\text{B}_5\text{Cl}_5]$  [39]; in each case, the trigonal bipyramidal  $\text{M}_2\text{B}_3$  unit is capped by two  $\text{BH}_3$  fragments over the  $\text{M}_2\text{B}$  faces. A comparison of the structural parameters and chemical shifts of these analogues is shown in Table 2. Another interesting molecule from group 5 is  $[(\text{Cp}^*\text{Ta})_2\text{B}_5\text{H}_{11}\text{Cl}_2]$  [23] having a contrasting geometry. It has a *nido* structure based on a *closo* dodecahedron by removing one five-connected vertex. Apart from these  $\text{M}_2\text{B}_5$  molecules, group 8 and 9 metals generate monometallic clusters *viz.*  $[(\eta^5\text{-C}_5\text{H}_5)\text{FeB}_5\text{H}_{10}]$  [57],  $[\text{Cp}^*\text{RuB}_5\text{H}_{10}]$  [58],  $[(\eta^5\text{-C}_5\text{H}_5)\text{CoB}_5\text{H}_9]$  [59] and  $[(\eta^5\text{-C}_5\text{Me}_5)\text{IrB}_5\text{H}_9]$  [60] showing interesting sandwich structures mimicking their organometallic counterpart ferrocene. These molecules provided an additional bridge between metallaborane and organometallic chemistry.

**Table 2.** Selected structural data and  $^{11}\text{B}$  chemical shifts of different  $\text{M}_2\text{B}_5$  clusters from Group 4–9 metals.

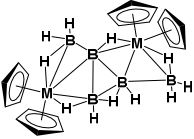
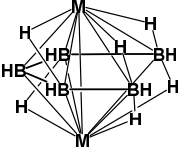
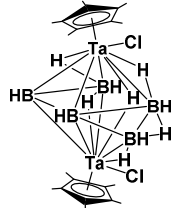
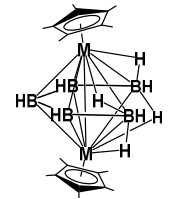
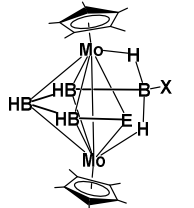
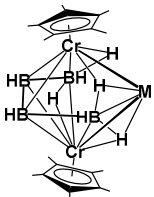
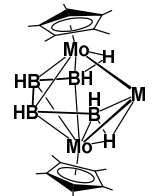
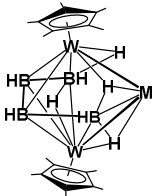
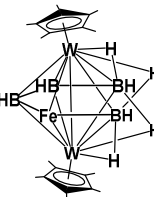
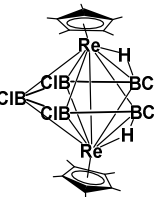
Metallaborane	Geometry	Sep <sup>a</sup>	Avg. <i>d</i> [M–M] (Å)	Avg. <i>d</i> [M–B] (Å)	Avg. <i>d</i> [B–B] (Å)	$^{11}\text{B}$ NMR (ppm)	Ref.
$[(\text{Cp}_2\text{M})_2\text{B}_5\text{H}_{11}]$ M = Zr, Hf		10	<sup>b</sup>	2.50(Zr) 2.50(Hf)	1.78(Zr) 1.78(Hf)	8.1, 2.5, −4.1 (Zr) −3.8, 2.0, 4.6 (Hf)	[55,56]
$[\text{M}_2\text{B}_5\text{H}_{11}]$ M = CpV, Cp*Ta		6	2.76 (V) 2.92 (Ta)	2.23 (V) 2.32 (Ta)	1.73 (V) 1.80 (Ta)	−1.8, 3.4, 21.9 (V) 3.7, 23.9, 44.7 (Ta)	[23,30]
$[\text{Cp}^*\text{TaB}_5\text{H}_{11}\text{Cl}_2]$		8	3.22	2.38	1.76	77.7, 18.8, 15, −10	[23]
$[(\text{Cp}^*\text{M})_2\text{B}_5\text{H}_9]$ M = Cr, Mo, W		6	2.62 (Cr) 2.80 (Mo) 2.81 (W)	2.15 (Cr) 2.24 (Mo) 2.23 (W)	1.67 (Cr) 1.72 (Mo) 1.71 (W)	25.0, 86.2, 91.5 (Cr) 62.9 (3 B), 25.8 (Mo) 26.8, 46.9, 49.2 (W)	[36–38,40]
$[(\text{Cp}^*\text{Mo})_2\text{B}_4\text{EH}_5\text{X}]$ E = S, Se; X = H E = Te; X = Cl		6	2.78 (S) 2.77 (Se) 2.84 (Te)	2.21 (S) 2.24 (Se) 2.17 (Te)	1.67 (S) 1.83 (Se) 1.69 (Te)	101.1, 76.7, 40.3, 10.1 (S) 100.7, 76.7, 41.8, 16.8 (Se) 95.5, 73.2, 40.7, 26.7 (Te)	[31]



Table 2. Cont.

Metallaborane	Geometry	Sep <sup>a</sup>	Avg. <i>d</i> [M–M] (Å)	Avg. <i>d</i> [M–B] (Å)	Avg. <i>d</i> [B–B] (Å)	<sup>11</sup> B NMR (ppm)	Ref.
[(Cp*Cr) <sub>2</sub> B <sub>4</sub> H <sub>8</sub> M] M = Fe(CO) <sub>3</sub> , Co <sub>2</sub> (CO) <sub>3</sub>		6	2.70 (Fe) 2.69 (Co.)	2.15 (Fe) 2.15 (Co.)	1.71 (Fe) 1.69 (Co.)	27.3, 80.0, 117.5 (Fe) 36.6, 57.5, 113.9, 121.7 (Co.)	[35]
[(Cp*Mo) <sub>2</sub> B <sub>4</sub> H <sub>4</sub> M] M = H <sub>2</sub> Cr(CO) <sub>4</sub> (5), H <sub>2</sub> W(CO) <sub>4</sub> , W(CO) <sub>5</sub>		6	2.82 (Cr) 2.82 (W) 2.83 (W)	2.27 (Cr) 2.23 (W) 2.23 (W)	1.72 (Cr) 1.71 (W) 1.72 (W)	83.5, 81.3, 41.3, 27.1 (Cr) 27.9, 41.9, 81.2 (W) 77.0, 77.9, 103.0 (W)	This Work, [49]
[(Cp*W) <sub>2</sub> B <sub>4</sub> H <sub>4</sub> M] M = Cr(CO) <sub>4</sub> (1), Mo(CO) <sub>4</sub> (2), W(CO) <sub>4</sub> (3)		6	2.84 (Cr) 2.83 (Mo) 2.89 (W)	2.38 (Cr) 2.27 (Mo) 2.24 (W)	1.73 (Cr) 1.71 (Mo) 1.71 (W)	70.6, 62.2, 36.5, 25.0 (Cr) 70.1, 60.1, 39.1, 25.6 (Mo) 70.2, 60.1, 35.5, 26.1 (W)	This work
[(Cp*W) <sub>2</sub> B <sub>4</sub> H <sub>8</sub> M] M = Fe(CO) <sub>3</sub> (4)		6	2.82	2.28	1.74	79.0, 76.2, 41.0, 35.9	This work
[(Cp*Re) <sub>2</sub> B <sub>5</sub> Cl <sub>5</sub> H <sub>2</sub> ]		6	2.76	2.20	1.74	28.1, 48.3, 88.3	[39]

<sup>a</sup> Skeletal electron pair count. <sup>b</sup> No M–M bond.

### 3. Materials and Methods

#### 3.1. General Procedures and Instrumentation

All the manipulations were conducted under an argon atmosphere using standard Schlenk techniques. Solvents were distilled prior to use under an argon atmosphere.  $[\text{Cp}^*\text{MoCl}_4]$ ,  $[\text{Cp}^*\text{WCl}_4]$ ,  $[\text{M}(\text{CO})_5\cdot\text{thf}]$  ( $\text{M} = \text{Cr}, \text{Mo}$  and  $\text{W}$ ) were prepared according to literature methods [61–63], while other chemicals, such as  $[\text{LiBH}_4]$  2.0 M in thf,  $\text{Cp}^*\text{H}$ ,  $n\text{-BuLi}$ ,  $[\text{Cr}(\text{CO})_6]$ ,  $[\text{Mo}(\text{CO})_6]$ ,  $[\text{W}(\text{CO})_6]$  and  $[\text{Fe}_2(\text{CO})_9]$  were obtained commercially (Sigma-Aldrich, St. Louis, MO, USA) and used as received. MeI was purchased from Aldrich and freshly distilled prior to use. The external reference for the  $^{11}\text{B}$  NMR,  $[\text{Bu}_4\text{N}(\text{B}_3\text{H}_8)]$  was synthesized with the literature method [64]. Preparative thin layer chromatography (TLC) was carried on 250 mm dia aluminum supported silica gel TLC plates (MERCK TLC Plates, Merck, Darmstadt, Germany). NMR spectra were recorded on 400 and 500 MHz Bruker FT-NMR spectrometer (Bruker, Billerica, MA, USA). The residual solvent protons were used as a reference ( $\delta$ , ppm,  $\text{CDCl}_3$ , 7.26), while a sealed tube containing  $[\text{Bu}_4\text{N}(\text{B}_3\text{H}_8)]$  in  $[\text{D}_6]$  [64] benzene ( $\delta_{\text{B}}$ , ppm,  $-30.07$ ) was used as an external reference for the  $^{11}\text{B}$  NMR. Infrared spectra were recorded on a Nicolet iS10 spectrometer (JASCO, Easton, MD, USA). The photo-reactions described in this report were conducted in a Luzchem LZC-4 V photo reactor (Luzchem, Ottawa, Canada), with irradiation at 254–350 nm. MALDI-TOF mass spectra were recorded on a Bruker Ultraflexxtreme (Bruker, Billerica, MA, USA) by using 2,5-dihydroxybenzoic acid as a matrix and a ground steel target plate.

**Synthesis of 1–3:** In a flame-dried Schlenk tube  $[\text{Cp}^*\text{WCl}_4]$ , (0.1 g, 0.22 mmol) in 15 mL of toluene was treated with a 5-fold excess of  $[\text{LiBH}_4\cdot\text{thf}]$  (0.55 mL, 1.1 mmol) at  $-78^\circ\text{C}$  and allowed to stir at room temperature for one hour. After removal of toluene, the residue was extracted into hexane and filtered through a frit using Celite. The brownish-green hexane extract was dried in vacuo, and taken in 15 mL of THF and heated at  $65^\circ\text{C}$  with  $[\text{M}(\text{CO})_5\cdot\text{thf}]$  ( $\text{M} = \text{Cr}, \text{Mo}$  and  $\text{W}$ ) for 22 h. The solvent was evaporated in vacuo and residue was extracted into hexane and passed through celite. After removal of solvent from the filtrate, the residue was subjected to chromatographic workup using silica gel TLC plates. Elution with a hexane/ $\text{CH}_2\text{Cl}_2$  (75:15 *v/v*) mixture yielded brown 1 (0.011 g, 6%) (in case of  $[\text{Cr}(\text{CO})_5\cdot\text{THF}]$ ) along with known  $[(\text{Cp}^*\text{W})_2\text{B}_5\text{H}_9]$  (0.048 g, 31%), greenish brown 2 (0.014 g, 7%) (in case of  $[\text{Mo}(\text{CO})_5\cdot\text{THF}]$ ) along with earlier reported  $[(\text{Cp}^*\text{W}(\text{CO})_2)_2\text{B}_2\text{H}_2\text{Mo}(\text{CO})_4]$  (0.028 g, 13%),  $[(\text{Cp}^*\text{W})_2\text{B}_5\text{H}_9]$  (0.050 g, 32%) and green 3 (0.013 g, 6%) (in case of  $[\text{W}(\text{CO})_5\cdot\text{thf}]$ ) along with earlier reported  $[(\text{Cp}^*\text{W}(\text{CO})_2)_2\text{B}_2\text{H}_2\text{W}(\text{CO})_4]$  (0.046 g, 20%) and  $[(\text{Cp}^*\text{W})_2\text{B}_5\text{H}_9]$  (0.044 g, 29%).

**1:**  $^{11}\text{B}\{^1\text{H}\}$  NMR (22  $^\circ\text{C}$ , 128 MHz,  $\text{CDCl}_3$ ):  $\delta$  = 70.6 (br, 1B), 62.2 (br, 1B), 36.5 (br, 1B), 25.0 (br, 1B);  $^1\text{H}$  NMR (22  $^\circ\text{C}$ , 400 MHz,  $\text{CDCl}_3$ ):  $\delta$  = 4.12 (br, 2H,  $\text{BH}_t$ ), 3.66 (br, 2H,  $\text{BH}_t$ ), 2.22 (s, 15H,  $\text{Cp}^*$ ), 2.21 (s, 15H,  $\text{Cp}^*$ ),  $-6.88$  (br, 1H,  $\text{W-H-B}$ ),  $-10.71$  (br, 1H,  $\text{W-H-B}$ ),  $-11.69$  (br, 1H,  $\mu_3\text{-H}$ ),  $-14.27$  (br, 1H,  $\mu_3\text{-H}$ ); IR (hexane)  $\nu/\text{cm}^{-1}$ : 2525 w( $\text{BH}_t$ ), 1922, 1855 w(CO).

**2:** HR-MS (high resolution mass spectrometry) ( $\text{ESI}^+$ ):  $m/z$  calculated for  $[\text{C}_{24}\text{H}_{38}\text{O}_4\text{B}_4\text{W}_2\text{Mo}+\text{K}]^+$ : 939.0853; found 939.0834;  $^{11}\text{B}\{^1\text{H}\}$  NMR (22  $^\circ\text{C}$ , 128 MHz,  $\text{CDCl}_3$ ):  $\delta$  = 70.1 (br, 1B), 60.1 (br, 1B), 39.1 (br, 1B), 25.6 (br, 1B);  $^1\text{H}$  NMR (22  $^\circ\text{C}$ , 400 MHz,  $\text{CDCl}_3$ ):  $\delta$  = 6.38 (br, 4H,  $\text{BH}_t$ ), 2.20 (s, 30H,  $\text{Cp}^*$ ),  $-6.21$  (br, 1H,  $\text{W-H-B}$ ),  $-8.53$  (br, 1H,  $\text{W-H-B}$ ),  $-11.06$  (br, 1H,  $\mu_3\text{-H}$ ),  $-13.0$  (br, 1H,  $\mu_3\text{-H}$ ); IR (hexane)  $\nu/\text{cm}^{-1}$ : 2482 w( $\text{BH}_t$ ), 2011, 1945, 1878 w(CO).

**3:** HR-MS ( $\text{ESI}^+$ ):  $m/z$  calculated for  $[\text{C}_{24}\text{H}_{38}\text{O}_4\text{B}_4\text{W}_3+\text{H}]^+$ : 987.1749; found 987.1727;  $^{11}\text{B}\{^1\text{H}\}$  NMR (22  $^\circ\text{C}$ , 128 MHz,  $\text{CDCl}_3$ ):  $\delta$  = 70.3 (br, 1B), 60.1 (br, 1B), 35.5 (br, 1B), 26.1 (br, 1B);  $^1\text{H}$  NMR (22  $^\circ\text{C}$ , 400 MHz,  $\text{CDCl}_3$ ):  $\delta$  = 6.05 (br, 2H,  $\text{BH}_t$ ), 5.78 (br, 2H,  $\text{BH}_t$ ), 2.18 (s, 30H,  $\text{Cp}^*$ ),  $-6.74$  (br, 1H,  $\text{W-H-B}$ ),  $-7.05$  (br, 1H,  $\text{W-H-B}$ ),  $-10.90$  (br, 1H,  $\mu_3\text{-H}$ ),  $-13.13$  (br, 1H,  $\mu_3\text{-H}$ ); IR (hexane)  $\nu/\text{cm}^{-1}$ : 2467 w( $\text{BH}_t$ ), 2028, 1984, 1926, 1878, 1835 w(CO).

**Synthesis of 4:** In a flame-dried Schlenk tube  $[\text{Cp}^*\text{WCl}_4]$ , (0.1 g, 0.22 mmol) in 15 mL of toluene was treated with a 5-fold excess of  $[\text{LiBH}_4\cdot\text{thf}]$  (0.55 mL, 1.1 mmol) at  $-78^\circ\text{C}$  and allowed to stir at room temperature for one hour. After removal of toluene, the residue was extracted into hexane and filtered

through a frit using Celite. The brownish-green hexane extract was dried in vacuo, and taken in 15 mL of THF and heated at 65 °C with  $\text{Fe}_2(\text{CO})_9$  for 22 h. The solvent was evaporated in vacuo and residue was extracted into hexane and passed through celite. After removal of solvent from the filtrate, the residue was subjected to chromatographic workup using silica gel TLC plates. Elution with a hexane/ $\text{CH}_2\text{Cl}_2$  (75:15 *v/v*) mixture yielded green 4 (0.020 g, 11%) along with known  $[(\text{Cp}^*\text{W})_2\text{B}_5\text{H}_9]$  (0.040 g, 26%).

**4:** HR-MS (ESI<sup>+</sup>): *m/z* calculated for  $[\text{C}_{23}\text{H}_{38}\text{O}_3\text{B}_4\text{W}_2\text{Fe}+\text{Na}]^+$ : 853.1459; found 853.1456;  $^{11}\text{B}\{^1\text{H}\}$  NMR (22 °C, 128 MHz,  $\text{CDCl}_3$ ):  $\delta$  = 79.0 (br, 1B), 76.2 (br, 1B), 41.0 (br, 1B), 35.8 (br, 1B);  $^1\text{H}$  NMR (22 °C, 400 MHz,  $\text{CDCl}_3$ ):  $\delta$  = 6.37, (br, 2H,  $\text{BH}_t$ ), 6.05, (br, 2H,  $\text{BH}_t$ ), 2.24 (s, 30H, Cp\*), −6.79 (br, 2H, W–H–B), −12.92 (br, 2H, W–H–B); IR (hexane)  $\nu/\text{cm}^{-1}$ : 2482 w( $\text{BH}_t$ ), 1984, 1918 w(CO).

**Synthesis of 5:** In a flame-dried Schlenk tube  $[\text{Cp}^*\text{MoCl}_4]$ , (0.1 g, 0.27 mmol) in 10 mL of toluene was treated with a 5-fold excess of  $[\text{LiBH}_4\cdot\text{thf}]$  (0.7 mL, 1.4 mmol) at −78 °C and allowed to stir at room temperature for one hour. After removal of toluene, the residue was extracted into hexane and filtered through a frit using Celite. The brownish-green hexane extract was dried in vacuo, and taken in 10 mL of THF and heated at 65 °C with  $[\text{Cr}(\text{CO})_5\cdot\text{thf}]$  for 18 hours. The solvent was evaporated in vacuo and residue was extracted into hexane and passed through celite. After removal of solvent from the filtrate, the residue was subjected to chromatographic workup using silica gel TLC plates. Elution with a hexane/ $\text{CH}_2\text{Cl}_2$  (80:10 *v/v*) mixture yielded dark brown 5 (0.026 g, 14%) along with known  $[(\text{Cp}^*\text{Mo})_2\text{B}_5\text{H}_9]$  (0.042 g, 29%).

**5:** HR-MS (ESI<sup>+</sup>): *m/z* calculated for  $[\text{C}_{24}\text{H}_{38}\text{O}_4\text{B}_4\text{Mo}_2\text{Cr}+\text{Na}]^+$ : 705.0553; found 705.0523;  $^{11}\text{B}\{^1\text{H}\}$  NMR (22 °C, 128 MHz,  $\text{CDCl}_3$ ):  $\delta$  = 83.5 (br, 1B), 81.3 (br, 1B), 41.3 (br, 1B), 27.1 (br, 1B);  $^1\text{H}$  NMR (22 °C, 400 MHz,  $\text{CDCl}_3$ ):  $\delta$  = 6.29, (br, 2H,  $\text{BH}_t$ ), 5.89, (br, 2H,  $\text{BH}_t$ ), 2.06 (s, 30H, 2Cp\*), −6.48 (br, 1H, Mo–H–B), −10.56 (br, 1H, Mo–H–B), −11.89 (br, 1H,  $\mu_3\text{-H}$ ), −15.42 (br, 1H,  $\mu_3\text{-H}$ ); IR (hexane)  $\nu/\text{cm}^{-1}$ : 2474 ( $\text{BH}_t$ ), 1996, 1941, 1886, 1851 (CO).

### 3.2. X-ray Structure Analysis

Single crystals of 1–5 suitable for X-ray diffraction were grown from hexane/ $\text{CH}_2\text{Cl}_2$  solution at −10 °C. Crystal data for 2, 3, 4 and 5 were collected and integrated using D8 VENTURE Bruker AXS single crystal diffractometer and for 1 Bruker Kappa apexII CCD single crystal diffractometer, equipped with graphite monochromated Mo  $\text{K}\alpha$  ( $\lambda$  = 0.71073 Å) radiation (details Table 3). Data collection for 1 was carried out at 296 K and for 2, 3, 4 and 5 at 150 K, using  $\omega$ – $\phi$  scan modes. Multi-scan absorption correction has been employed for the data using SADABS [65–67] program. The structures were solved by heavy atom methods using SHELXS-97 or SIR92 [65–67] and refined using SHELXL-2014 [65–67]. The structures were drawn using Olex2 [68]. Crystallographic data have been deposited with the Cambridge Crystallographic Data Center as supplementary publication no. CCDC-1893708 (1), CCDC-1893709 (2), CCDC-1893711 (3), CCDC-1893712 (4) and CCDC-1893713 (5) (see Supplementary Materials). These data can be obtained free of charge from The Cambridge Crystallographic Data Centre via [www.ccdc.cam.ac.uk/data\\_request/cif](http://www.ccdc.cam.ac.uk/data_request/cif).

**Table 3.** Crystallographic data and structure refinement information for 1–5.

	1	2	3	4	5
Empirical formula	C <sub>24</sub> H <sub>37</sub> B <sub>4</sub> O <sub>4</sub> CrW <sub>2</sub>	C <sub>24</sub> H <sub>30</sub> B <sub>4</sub> O <sub>4</sub> MoW <sub>2</sub>	C <sub>24</sub> H <sub>30</sub> B <sub>4</sub> O <sub>4</sub> W <sub>3</sub>	C <sub>23</sub> H <sub>38</sub> B <sub>4</sub> O <sub>3</sub> FeW <sub>2</sub>	C <sub>24</sub> H <sub>38</sub> B <sub>4</sub> O <sub>4</sub> CrMo <sub>2</sub>
Formula weight	852.47	889.36	977.27	829.32	677.66
Crystal system	Orthorhombic	Triclinic	Triclinic	Monoclinic	Monoclinic
Space group	<i>Pca</i> 21	<i>P</i> −1	<i>P</i> −1	<i>P</i> 2 <sub>1</sub> / <i>n</i>	<i>P</i> 2 <sub>1</sub> / <i>c</i>
<i>a</i> (Å)	23.323(5)	16.3096(16)	16.8420(15)	11.6885(13)	19.454(2)
<i>b</i> (Å)	14.555(3)	18.8186(18)	19.051(2)	16.2795(16)	13.2430(11)
<i>c</i> (Å)	17.009(7)	19.9272(18)	19.390(2)	15.0773(17)	21.905(2)
$\alpha$ (°)	90	85.532(3)	85.443(4)	90	90
$\beta$ (°)	90.000(10)	71.947(3)	79.671(3)	110.538(4)	94.494(4)
$\gamma$ (°)	90	89.111(3)	70.858(3)	90	90
<i>V</i> (Å <sup>3</sup> )	5774(3)	5797.1(10)	5780.6(10)	2686.6(5)	5626.2(9)
<i>Z</i>	8	8	8	4	8
<i>D</i> <sub>calc</sub> (g/cm <sup>3</sup> )	1.961	2.038	2.246	2.050	1.600
<i>F</i> (000)	3240	3328	3584	1576	2736
$\mu$ (mm <sup>−1</sup> )	8.346	8.370	11.937	9.097	1.285
$\theta$ Range (°)	3.2–22.1	2.27–27.51	2.26–27.50	2.50–27.52	2.57–27.46
no. of reflns collected	8977	26525	26460	6147	12768
no. of unique reflns [ <i>I</i> > 2 $\sigma$ ( <i>I</i> )]	3645	22650	22550	5606	10014
goodness-of-fit on <i>F</i> <sup>2</sup>	0.997	1.065	1.104	1.063	1.018
final <i>R</i> indices [ <i>I</i> > 2 $\sigma$ ( <i>I</i> )]	<i>R</i> 1 = 0.0879, <i>wR</i> 2 = 0.1580	<i>R</i> 1 = 0.0349, <i>wR</i> 2 = 0.0819	<i>R</i> 1 = 0.0965, <i>wR</i> 2 = 0.1988	<i>R</i> 1 = 0.0379, <i>wR</i> 2 = 0.1175	<i>R</i> 1 = 0.0810, <i>wR</i> 2 = 0.1827
<i>R</i> indices (all data)	<i>R</i> 1 = 0.2386, <i>wR</i> 2 = 0.2215	<i>R</i> 1 = 0.0458, <i>wR</i> 2 = 0.0880	<i>R</i> 1 = 0.1133, <i>wR</i> 2 = 0.2103	<i>R</i> 1 = 0.0421, <i>wR</i> 2 = 0.1236	<i>R</i> 1 = 0.1054, <i>wR</i> 2 = 0.2014

#### 4. Conclusions

In summary, we have described the synthesis of various homo and heterometallic tungstaborane clusters  $[(Cp^*W)_2B_4H_8M]$ , **1–4** (**1**:  $M = Cr(CO)_4$ ; **2**:  $M = Mo(CO)_4$ ; **3**:  $M = W(CO)_4$ ; **4**:  $M = Fe(CO)_3$ ) with different metal carbonyl fragments. Reaction of  $[Cp^*MoCl_4]$  and  $[Cr(CO)_5 \cdot thf]$  yielded the mixed-metal molybdaborane cluster  $[(Cp^*Mo)_2B_4H_8Cr(CO)_4]$ , **5**. Compounds **1–5** are analogous to their parent tungstaborane/molybdaborane  $[(Cp^*M)_2B_5H_9]$  ( $M = W, Mo$ ) that seem to have been generated by the replacement of one  $\{BH\}$  vertex from  $[(Cp^*W)_2B_5H_9]$  or  $[(Cp^*Mo)_2B_5H_9]$  (in case of **5**). One of the major differences in these molecules is the position of the  $Fe(CO)_3$  unit in compound **4**. While in **1–3** the metal carbonyl fragment caps one of the  $\{W_2B\}$  triangular faces, in compound **4**,  $Fe(CO)_3$  is part of the triangular  $\{W_2Fe\}$  faces. This type of  $M_2B_5$  molecule is rare. These results further demonstrate the use of metal carbonyls to generate molecular clusters that show exciting geometry and bonding interactions.

**Supplementary Materials:** The following are available online at <http://www.mdpi.com/2304-6740/7/3/27/s1>. It contains  $^1H$ ,  $^{11}B\{^1H\}$ ,  $^{13}C\{^1H\}$  NMR and mass spectra; X-ray analysis details and CIF and the checkCIF.

**Author Contributions:** R.B. (Ranjit Bag) and S.S. conceived and designed the experiment; R.B. (Ranjit Bag) and S.S. performed the synthesis and the spectroscopic analysis; results were discussed with R.B. (Rosmita Borthakur), B.M. and S.G.; R.B. (Rosmita Borthakur) prepared the manuscript with feedback from S.G. and J.-F.H.; S.G. supervision, S.G. project administration. T.R., V.D. and J.-F.H. performed the X-ray analysis.

**Funding:** This research was funded by Council of Scientific & Industrial Research (CSIR) (Project No. 01(2939)/18/emr-ii), New Delhi, India.

**Acknowledgments:** R.B. (Ranjit Bag) thanks IIT Madras, S.S. thanks Science and Engineering Research Board (SERB).

**Conflicts of Interest:** The authors declare no conflict of interest.

#### References

1. Fehlnner, T.P.; Halet, J.-F.; Saillard, J.-Y. *Molecular Clusters: A Bridge to Solid-State Chemistry*; Cambridge University Press: Cambridge, UK, 2007.
2. Greenwood, N.N.; Ward, I.M. Metalloboranes and metal–boron bonding. *Chem. Soc. Rev.* **1974**, *3*, 231–271. [CrossRef]
3. Grimes, R.N. Structure and stereochemistry in metalloboron cage compounds. *Acc. Chem. Res.* **1978**, *11*, 420–427. [CrossRef]
4. Grimes, R.N. Metallacarboranes and metal–boron clusters in organometallic synthesis. *Pure Appl. Chem.* **1982**, *54*, 43–58. [CrossRef]
5. Barton, L.; Srivastava, D.K. *Comprehensive Organometallic Chemistry II*; Abel, E., Stone, F.G.A., Wilkinson, G.E., Eds.; Pergamon: New York, NY, USA, 1995; Volume 1, pp. 275–373.
6. Grimes, R.N. *Metal Interactions with Boron Clusters*; Plenum: New York, NY, USA, 1982; pp. 269–319. [CrossRef]
7. Cotton, F.A.; Murillo, C.A.; Wang, X. Low-Valent Ditantalum Complex  $Ta_2(\mu-BH_3)(\mu-dmpm)_3(\eta^2-BH_4)_2$ : First Dinuclear Compound Containing a Bridging  $BH_3$  Group with Direct Ta–B Bonds. *J. Am. Chem. Soc.* **1998**, *120*, 9594–9599. [CrossRef]
8. Kennedy, J.D. The Polyhedral Metallaboranes. *Prog. Inorg. Chem.* **1984**, *32*, 519–670.
9. Kennedy, J.D. The polyhedral metallaboranes, Part II, Metallaborane clusters with eight vertices and more. *Prog. Inorg. Chem.* **1986**, *34*, 211–434.
10. Kennedy, J.D. *Disobedient Skeletons*; Casanova, J., Ed.; Wiley: New York, NY, USA, 1998.
11. Pipal, J.R.; Grimes, R.N. Crystal structure of a tetracobalt tetraboron cluster,  $(\eta^5-C_5H_5)_4Co_4B_4H_4$ . Structural patterns in eight-vertex polyhedra. *Inorg. Chem.* **1979**, *18*, 257–263. [CrossRef]
12. Housecroft, C.E.; Fehlnner, T.P. Metalloboranes: Their Relationships to Metal–Hydrocarbon Complexes and Clusters. *Adv. Organomet. Chem.* **1982**, *21*, 57–112. [CrossRef]
13. Grimes, R.N. Boron Clusters Come of Age. *J. Chem. Educ.* **2004**, *81*, 657–672. [CrossRef]
14. Grimes, R.N. *Comprehensive Organometallic Chemistry II*; Abel, E., Stone, F.G.A., Wilkinson, G., Eds.; Pergamon: New York, NY, USA, 1995; Volume 1, Chapter 9.

15. Gaines, D.F. *Recent Advances in the Chemistry of Pentaborane (9)*; Parry, R.W., Kodama, G., Eds.; Pergamon: Oxford, UK, 1980.
16. Shore, S.G.; Jan, D.-Y.; Hsu, L.-Y.; Hsu, W.-L. Insertion of boron into an osmium–carbonyl bond. Preparation and structure of the carbonyl borylidyne  $(\mu\text{-H})_3(\text{CO})_9\text{Os}_3\text{BCO}$ . *J. Am. Chem. Soc.* **1983**, *105*, 5923–5924. [[CrossRef](#)]
17. Jan, D.-Y.; Workman, D.P.; Hsu, L.-Y.; Krause, J.A.; Shore, S.G. Clusters derived from the hydroboration of decacarbonyldi- $\mu$ -hydridotriosmium and their derivatives. *Inorg. Chem.* **1992**, *31*, 5123–5131. [[CrossRef](#)]
18. Leyden, R.N.; Sullivan, B.P.; Baker, R.T.; Hawthorne, M.F. Synthesis of closo- and nido-metallaboranes from metallocenes. *J. Am. Chem. Soc.* **1978**, *100*, 3758–3765. [[CrossRef](#)]
19. Lupan, A.; King, R.B. Boron in Organometallic Chemistry. In *Handbook of Boron Science with Applications in Organometallics, Catalysis, Materials and Medicine*; Hosmane, N.S., Eagling, R., Eds.; World Scientific: London, UK, 2018; Volume 1, Chapter 1; pp. 1–20.
20. Hosmane, N.S. *Boron Science: New Technologies and Applications*; CRC Press, Taylor and Francis Group: Boca Raton, FL, USA, 2011.
21. Weller, A.S. *Comprehensive Organometallic Chemistry III*; Mingos, D.M.P., Crabtree, R.H., Eds.; Pergamon: New York, NY, USA, 2007; Volume 3, Chapter 3.04; pp. 133–174.
22. Hosmane, N.S.; Maguire, J.A. *Comprehensive Organometallic Chemistry III*; Mingos, D.M.P., Crabtree, R.H., Eds.; Pergamon: New York, NY, USA, 2007; Volume 3, Chapter 3.05; pp. 175–264.
23. Bose, S.K.; Geetharani, K.; Varghese, B.; Mobin, S.M.; Ghosh, S. Metallaboranes of the Early Transition Metals: Direct Synthesis and Characterization of  $[(\eta^5\text{-C}_5\text{Me}_5)\text{Ta}]_2\text{B}_n\text{H}_m$  ( $n = 4, m = 10$ ;  $n = 5, m = 11$ ),  $[(\eta^5\text{-C}_5\text{Me}_5)\text{Ta}]_2\text{B}_5\text{H}_{10}(\text{C}_6\text{H}_4\text{CH}_3)$ , and  $[(\eta^5\text{-C}_5\text{Me}_5)\text{TaCl}]_2\text{B}_5\text{H}_{11}$ . *Chem. Eur. J.* **2008**, *14*, 9058–9064. [[CrossRef](#)] [[PubMed](#)]
24. Sahoo, S.; Reddy, K.H.K.; Dhayal, R.S.; Mobin, S.M.; Ramkumar, V.; Jemmis, E.D.; Ghosh, S. Chlorinated Hypoelectronic Dimetallaborane Clusters: Synthesis, Characterization, and Electronic Structures of  $(\eta^5\text{-C}_5\text{Me}_5\text{W})_2\text{B}_5\text{H}_n\text{Cl}_m$  ( $n = 7, m = 2$  and  $n = 8, m = 1$ ). *Inorg. Chem.* **2009**, *48*, 6509–6516. [[CrossRef](#)] [[PubMed](#)]
25. Sahoo, S.; Dhayal, R.S.; Varghese, B.; Ghosh, S. Unusual Open Eight-Vertex Oxamolybdaboranes: Structural Characterizations of  $(\eta^5\text{-C}_5\text{Me}_5\text{Mo})_2\text{B}_5(\mu_3\text{-OEt})\text{H}_6\text{R}$  ( $\text{R} = \text{H}$  and  $n\text{-BuO}$ ). *Organometallics* **2009**, *28*, 1586–1589. [[CrossRef](#)]
26. Geetharani, K.; Bose, S.K.; Pramanik, G.; Saha, T.K.; Ramkumar, V.; Ghosh, S. An Efficient Route to Group 6 and 8 Metallaborane Compounds: Synthesis of arachno- $[\text{Cp}^*\text{Fe}(\text{CO})\text{B}_3\text{H}_8]$  and closo- $[(\text{Cp}^*\text{M})_2\text{B}_5\text{H}_9]$  ( $\text{M} = \text{Mo}, \text{W}$ ). *Eur. J. Inorg. Chem.* **2009**, 1483–1487. [[CrossRef](#)]
27. Dhayal, R.S.; Chakrahari, K.K.V.; Ramkumar, V.; Ghosh, S. B-Alkylation and Arylation of  $[(\eta^5\text{-C}_5\text{Me}_5\text{Mo})_2\text{B}_5\text{H}_9]$ : Synthesis and Characterization of Isomeric  $[(\eta^5\text{-C}_5\text{Me}_5\text{Mo})_2\text{B}_5\text{H}_{9-n}\text{R}_n]$  (When  $\text{R} = n\text{-Bu}$ ,  $n = 2, 1$ ;  $\text{R} = \text{Ph}$ ,  $n = 2, 1$ ). *J. Clust. Sci.* **2009**, *20*, 565–572. [[CrossRef](#)]
28. Sahoo, S.; Mobin, S.M.; Ghosh, S. Direct insertion of sulfur, selenium and tellurium atoms into metallaborane cages using chalcogen powders. *J. Organomet. Chem.* **2010**, *695*, 945–949. [[CrossRef](#)]
29. Bose, S.K.; Geetharani, K.; Ghosh, S. C–H activation of arenes and heteroarenes by early transition metallaborane,  $[(\text{Cp}^*\text{Ta})_2\text{B}_5\text{H}_{11}]$  ( $\text{Cp}^* = \eta^5\text{-C}_5\text{Me}_5$ ). *Chem. Commun.* **2011**, *47*, 11996–11998. [[CrossRef](#)] [[PubMed](#)]
30. Roy, D.K.; Bose, S.K.; Geetharani, K.; Chakrahari, K.K.V.; Mobin, S.M.; Ghosh, S. Synthesis and Structural Characterization of New Divanada- and Diniobaboranes Containing Chalcogen Atoms. *Chem. Eur. J.* **2012**, *18*, 9983–9991. [[CrossRef](#)] [[PubMed](#)]
31. Chakrahari, K.K.; Thakur, A.; Mondal, B.; Ramkumar, V.; Ghosh, S. Hypoelectronic Dimetallaheteroboranes of Group 6 Transition Metals Containing Heavier Chalcogen Elements. *Inorg. Chem.* **2013**, *52*, 7923–7932. [[CrossRef](#)] [[PubMed](#)]
32. Chakrahari, K.K.; Thakur, A.; Anju, V.P.; Ghosh, S. B–H bond iodination of polyhedral dimolybdaborane and dimolybdathiaborane clusters. *J. Organomet. Chem.* **2014**, *751*, 321–325. [[CrossRef](#)]
33. Bag, R.; Mondal, B.; Bakthavachalam, K.; Roisnel, T.; Ghosh, S. Heterometallic boride clusters: Synthesis and characterization of butterfly and square pyramidal boride clusters. *Pure Appl. Chem.* **2018**, *90*, 665–675. [[CrossRef](#)]
34. Hashimoto, H.; Shang, M.; Fehlner, T.P. Clusters as Ligands. Coordination of an Electronically Unsaturated Chromaborane to an Iron Tricarbonyl Fragment. *J. Am. Chem. Soc.* **1996**, *118*, 8164–8165. [[CrossRef](#)]



35. Aldridge, S.; Hashimoto, H.; Kawamura, K.; Shang, M.; Fehlner, T.P. Cluster Expansion Reactions of Group 6 Metallaboranes. Syntheses, Crystal Structures, and Spectroscopic Characterizations of  $(\text{Cp}^*\text{Cr})_2\text{B}_5\text{H}_9$ ,  $(\text{Cp}^*\text{Cr})_2\text{B}_4\text{H}_8\text{Fe}(\text{CO})_3$ ,  $(\text{Cp}^*\text{Cr})_2\text{B}_4\text{H}_7\text{Co}(\text{CO})_3$ , and  $(\text{Cp}^*\text{Mo})_2\text{B}_5\text{H}_9\text{Fe}(\text{CO})_3$ . *Inorg. Chem.* **1998**, *37*, 928–940. [[CrossRef](#)]
36. Aldridge, S.; Fehlner, T.P.; Shang, M. Directed Synthesis of Chromium and Molybdenum Metallaborane Clusters. Preparation and Characterization of  $(\text{Cp}^*\text{Cr})_2\text{B}_5\text{H}_9$ ,  $(\text{Cp}^*\text{Mo})_2\text{B}_5\text{H}_9$ , and  $(\text{Cp}^*\text{MoCl})_2\text{B}_4\text{H}_{10}$ . *J. Am. Chem. Soc.* **1997**, *119*, 2339–2340. [[CrossRef](#)]
37. Aldridge, S.; Shang, M.; Fehlner, T.P. Synthesis of Novel Molybdaboranes from  $(\eta^5\text{-C}_5\text{R}_5)\text{MoCl}_n$  Precursors ( $\text{R} = \text{H}, \text{Me}; n = 1, 2, 4$ ). *J. Am. Chem. Soc.* **1998**, *120*, 2586–2598. [[CrossRef](#)]
38. Kim, D.Y.; Girolami, G.S. Synthesis and Characterization of the Octahydrotriborate Complexes  $\text{Cp}^*\text{V}(\text{B}_3\text{H}_8)_2$  and  $\text{Cp}^*\text{Cr}(\text{B}_3\text{H}_8)_2$  and the Unusual Cobaltaborane Cluster  $\text{Cp}^*_2\text{Co}_2(\text{B}_6\text{H}_{14})$ . *J. Am. Chem. Soc.* **2006**, *128*, 10969–10977. [[CrossRef](#)] [[PubMed](#)]
39. Guennic, B.L.; Jiao, H.; Kahlal, S.; Saillard, J.-Y.; Halet, J.-F.; Ghosh, S.; Shang, M.; Beatty, A.M.; Rheingold, A.L.; Fehlner, T.P. Synthesis and Characterization of Hypoelectronic Rhenaboranes. Analysis of the Geometric and Electronic Structures of Species Following Neither Borane nor Metal Cluster Electron-Counting Paradigms. *J. Am. Chem. Soc.* **2004**, *126*, 3203–3217. [[CrossRef](#)] [[PubMed](#)]
40. Weller, A.S.; Shang, M.; Fehlner, T.P. Synthesis of Mono- and Ditungstaboranes from Reaction of  $\text{Cp}^*\text{WCl}_4$  and  $[\text{Cp}^*\text{WCl}_2]_2$  with  $\text{BH}_3\cdot\text{thf}$  or  $\text{LiBH}_4$  ( $\text{Cp}^* = \eta^5\text{-C}_5\text{Me}_5$ ). Control of Reaction Pathway by Choice of Monoboron Reagent and Oxidation State of Metal Center. *Organometallics* **1999**, *18*, 53–64. [[CrossRef](#)]
41. Bullick, H.J.; Grebenik, P.D.; Green, M.L.H.; Hughes, A.K.; Leach, J.B.; McGowan, P.C. Synthesis of  $\eta$ -cyclopentadienyl-polyborane derivatives of molybdenum and tungsten. *J. Chem. Soc. Dalton Trans.* **1995**, 67–75. [[CrossRef](#)]
42. Aldridge, S.; Shang, M.; Fehlner, T.P. Origins of Unsaturation in Group 6 Metallaboranes. Synthesis, Crystal Structure, and Molecular Orbital Calculations for  $(\text{Cp}^*\text{MoCl})_2\text{B}_3\text{H}_7$  ( $\text{Cp}^* = \text{Pentamethylcyclopenta-dienyl}$ ). *J. Am. Chem. Soc.* **1997**, *119*, 11120–11121. [[CrossRef](#)]
43. Aldridge, S.; Hashimoto, H.; Shang, M.; Fehlner, T.P.  $\text{Cp}^*\text{TaCl}_2\text{B}_4\text{H}_8$ : Synthesis, crystal structure and spectroscopic characterization of an air-stable, electronically unsaturated, chiral tantalaborane. *J. Chem. Soc. Chem. Commun.* **1998**, 207–208. [[CrossRef](#)]
44. Bose, S.K.; Geetharani, K.; Varghese, B.; Ghosh, S. Condensed Tantalaborane Clusters: Synthesis and Structures of  $[(\text{Cp}^*\text{Ta})_2\text{B}_5\text{H}_7\{\text{Fe}(\text{CO})_3\}_2]$  and  $[(\text{Cp}^*\text{Ta})_2\text{B}_5\text{H}_9\{\text{Fe}(\text{CO})_3\}_4]$ . *Inorg. Chem.* **2011**, *50*, 2445–2449. [[CrossRef](#)] [[PubMed](#)]
45. Geetharani, K.; Krishnamoorthy, B.S.; Kahlal, S.; Mobin, S.M.; Halet, J.-F.; Ghosh, S. Synthesis and Characterization of Hypoelectronic Tantalaboranes: Comparison of the Geometric and Electronic Structures of  $[(\text{Cp}^*\text{TaX})_2\text{B}_5\text{H}_{11}]$  ( $\text{X} = \text{Cl}, \text{Br}, \text{and I}$ ). *Inorg. Chem.* **2012**, *51*, 10176–10184. [[CrossRef](#)] [[PubMed](#)]
46. Yuvaraj, K.; Roy, D.K.; Geetharani, K.; Mondal, B.; Anju, V.P.; Shankhari, P.; Ramkumar, V.; Ghosh, S. Chemistry of Homo- and Heterometallic Bridged-Borylene Complexes. *Organometallics* **2013**, *32*, 2705–2712. [[CrossRef](#)]
47. Anju, R.S.; Saha, K.; Mondal, B.; Dorcet, V.; Roisnel, T.; Halet, J.-F.; Ghosh, S. Chemistry of Diruthenium Analogue of Pentaborane(9) With Heterocumulenes: Toward Novel Trimetallic Cubane-Type Clusters. *Inorg. Chem.* **2014**, *53*, 10527–10535. [[CrossRef](#)] [[PubMed](#)]
48. Geetharani, K.; Bose, S.K.; Sahoo, S.; Varghese, B.; Mobin, S.M.; Ghosh, S. Cluster Expansion Reactions of Group 6 and 8 Metallaboranes Using Transition Metal Carbonyl Compounds of Groups 7–9. *Inorg. Chem.* **2011**, *50*, 5824–5832. [[CrossRef](#)] [[PubMed](#)]
49. Mondal, B.; Bag, R.; Roisnel, T.; Ghosh, S. Use of Single Metal Fragments for Cluster Building: Synthesis, Structure and Bonding of Heterometalla-boranes. *Inorg. Chem.* **2019**, *58*, 2744–2754. [[CrossRef](#)] [[PubMed](#)]
50. Mondal, B.; Bag, R.; Ghorai, S.; Bakthavachalam, K.; Jemmis, E.D.; Ghosh, S. Synthesis, Structure, Bonding, and Reactivity of Metal Complexes Comprising Diborane(4) and Diborene(2):  $[(\text{Cp}^*\text{Mo}(\text{CO})_2)_2\{\mu\text{-}\eta^2\text{-}\eta^2\text{-B}_2\text{H}_4\}]$  and  $[(\text{Cp}^*\text{M}(\text{CO})_2)_2\text{B}_2\text{H}_2\text{M}(\text{CO})_4]$ ,  $\text{M} = \text{Mo}, \text{W}$ . *Angew. Chem. Int. Ed.* **2018**, *57*, 8079–8083. [[CrossRef](#)] [[PubMed](#)]
51. Ghosh, S.; Lei, X.; Cahill, C.L.; Fehlner, T.P. Symmetrical Scission of the Coordinated Tetraborane in  $[(\text{Cp}^*\text{ReH}_2)_2\text{B}_4\text{H}_4]$  on CO Addition and Reassociation of the Coordinated Diboranes on  $\text{H}_2$  Loss. *Angew. Chem. Int. Ed.* **2000**, *39*, 2900–2902. [[CrossRef](#)]



52. Wade, K. Structural and Bonding Patterns in Cluster Chemistry. *Adv. Inorg. Chem. Radiochem.* **1976**, *18*, 1–66. [[CrossRef](#)]
53. Mingos, D.M.P. Polyhedral skeletal electron pair approach. *Acc. Chem. Res.* **1984**, *17*, 311–319. [[CrossRef](#)]
54. Jemmis, E.D.; Balakrishnarajan, M.N.; Pancharatna, P.D. Electronic Requirements for Macropolyhedral Boranes. *Chem. Rev.* **2002**, *102*, 93–144. [[CrossRef](#)] [[PubMed](#)]
55. Roy, D.K.; Mondal, B.; De, A.; Panda, S.; Ghosh, S. Novel Neutral Zirconaborane [(Cp<sub>2</sub>Zr)<sub>2</sub>B<sub>5</sub>H<sub>11</sub>]: An arachno-B<sub>3</sub>H<sub>9</sub> Analogue (Cp = η<sup>5</sup>-C<sub>5</sub>H<sub>5</sub>). *Organometallics* **2015**, *34*, 908–912. [[CrossRef](#)]
56. De, A.; Zhang, Q.-F.; Mondal, B.; Cheung, L.F.; Kar, S.; Saha, K.; Varghese, B.; Wang, L.-S.; Ghosh, S. [(Cp<sub>2</sub>M)<sub>2</sub>B<sub>9</sub>H<sub>11</sub>] (M = Zr or Hf): Early transition metal ‘guarded’ heptaborane with strong covalent and electrostatic bonding. *Chem. Sci.* **2018**, *9*, 1976–1981. [[CrossRef](#)] [[PubMed](#)]
57. Weiss, R.; Grimes, R.N. Polyhedral ferraboranes derived from the B<sub>5</sub>H<sub>8</sub><sup>−</sup> ion. Analogs of ferrocene, hexaborane(10), and nido-B<sub>11</sub>H<sub>15</sub>. *Inorg. Chem.* **1979**, *18*, 3291–3294. [[CrossRef](#)]
58. Ghosh, S.; Noll, B.C.; Fehlner, T.P. Borane Mimics of Classic Organometallic Compounds: [(Cp\*<sub>2</sub>Ru)B<sub>8</sub>H<sub>14</sub>(RuCp\*)]<sup>0,+</sup>, Isoelectronic Analogues of Dinuclear Pentalene Complexes. *Angew. Chem. Int. Ed.* **2005**, *44*, 6568–6571. [[CrossRef](#)] [[PubMed](#)]
59. Wilczynski, R.; Sneddon, L.G. Synthesis of two new cobaltaborane complexes: 1-(η<sup>5</sup>-C<sub>5</sub>H<sub>5</sub>)CoB<sub>5</sub>H<sub>9</sub> and 2-(η<sup>5</sup>-C<sub>5</sub>H<sub>5</sub>)CoB<sub>9</sub>H<sub>13</sub>. *Inorg. Chem.* **1979**, *18*, 864–866. [[CrossRef](#)]
60. Ghosh, S.; Noll, B.C.; Fehlner, T.P. Expansion of iridaborane clusters by addition of monoborane. Novel metallaboranes and mechanistic detail. *Dalton Trans.* **2008**, 371–378. [[CrossRef](#)]
61. Dhayal, R.S.; Sahoo, S.; Ramkumar, V.; Ghosh, S. Substitution at boron in molybdaborane frameworks: Synthesis and characterization of isomeric (η-C<sub>5</sub>Me<sub>5</sub>Mo)<sub>2</sub>B<sub>5</sub>H<sub>n</sub>X<sub>m</sub> (when X = Cl: n = 5, 7, 8; m = 4, 2, 1 and X = Me: n = 6, 7; m = 3, 2). *J. Organomet. Chem.* **2009**, *694*, 237–243. [[CrossRef](#)]
62. Green, M.L.H.; Hubert, J.D.; Mountford, P. Synthesis of the W≡W triply bonded dimers [W<sub>2</sub>(η<sup>5</sup>-C<sub>5</sub>H<sub>4</sub>R)<sub>2</sub>X<sub>4</sub>] (X = Cl, R = Me or Pri; X = Br, R = Pri) and X-ray crystal structures of [W(η<sup>5</sup>-C<sub>5</sub>H<sub>4</sub>Pri)Cl<sub>4</sub>] and [W<sub>2</sub>(η-C<sub>5</sub>H<sub>4</sub>Pri)<sub>2</sub>Cl<sub>4</sub>]. *J. Chem. Soc. Dalton Trans.* **1990**, 3793–3800. [[CrossRef](#)]
63. Kaushika, M.; Singh, A.; Kumar, M. The chemistry of group-VIb metal carbonyls. *Eur. J. Chem.* **2012**, *3*, 367–394. [[CrossRef](#)]
64. Ryschkewitsch, G.E.; Nainan, K.C. Octahydrotriborate(1−) [B<sub>3</sub>H<sub>8</sub>] salt. *Inorg. Synth.* **1974**, *15*, 113–114. [[CrossRef](#)]
65. Bruker. APEX2, SAINT and SADABS; Bruker AXS Inc.: Madison, WI, USA, 2004.
66. Sheldrick, G.M. SHELXS-97; University of Göttingen: Göttingen, Germany, 1997.
67. Sheldrick, G.M. Crystal structure refinement with SHELXL. *Acta Cryst.* **2015**, *71*, 3–8.
68. Dolomanov, O.V.; Bourhis, L.J.; Gildea, R.J.; Howard, J.A.K.; Puschmann, H. OLEX2: A complete structure solution, refinement and analysis program. *J. Appl. Cryst.* **2009**, *42*, 339–341. [[CrossRef](#)]

